Water Resources Research

RESEARCH ARTICLE
10.1029/2024WR039382

Contribution of Chemical Stratification to the Extent of Water Renewal in a Deep Lake

Giulia Valerio[1] and Marco Pilotti[1]

[1]DICATAM, Department of Civil, Environmental, Architectural Engineering and Mathematics, Università degli Studi di Brescia, Brescia, Italy

Key Points:

- A procedure to quantify the resistance to deep mixing in a chemically stratified lake is shown
- The chemical stratification induced by mineralization in deep eutrophic lakes may inhibit full circulations
- Deep warming will likely foster occasional mixing in chemically stratified lakes

Correspondence to:
G. Valerio,
giulia.valerio@unibs.it

Citation:
Valerio, G., & Pilotti, M. (2025). Contribution of chemical stratification to the extent of water renewal in a deep lake. *Water Resources Research*, *61*, e2024WR039382. https://doi.org/10.1029/2024WR039382

Received 6 NOV 2024
Accepted 27 JUN 2025

Author Contributions:
Conceptualization: Giulia Valerio, Marco Pilotti
Data curation: Giulia Valerio
Formal analysis: Giulia Valerio, Marco Pilotti
Investigation: Giulia Valerio
Methodology: Giulia Valerio, Marco Pilotti
Supervision: Marco Pilotti
Visualization: Giulia Valerio
Writing – original draft: Giulia Valerio
Writing – review & editing: Giulia Valerio, Marco Pilotti

Abstract Turnover events in deep lakes are crucial for water quality and trophic balance. If on one side there is wide consensus that climate change will strengthen the thermal stability of the epilimnion, on the other a smaller number of studies have investigated the stabilization operated by the chemical stratification, and the conditions under which it may occasionally fail. In this paper we investigate the role of thermal and trophic-induced stratification on the deep mixing of Lake Iseo, a pre-alpine lake that used to be monomictic in the past. The coupling of a site–specific density equation to 9 years of high-resolution temperature and wind data made it possible to compute the time series of the resistance to upwelling of deep waters and to quantify the role of the chemical stability. We show that the presence of calcium, bicarbonate and sulfate ions in the bottom layers, and the related increase in stability of about 10^3 Jm^{-2}, has hindered the occurrence of a deep overturn, even in presence of a thermally uniform water column. A full upwelling was thus inhibited in 3 of the observed winters, when it would otherwise have occurred. On the other hand, whereas our computations show that a destabilizing effect of possible future stronger winds is unlikely, the progressive deep-water warming that followed the isolation of the monimolimnion has strongly decreased the lake's thermal stability, counteracting the chemical stratification and progressively increasing the probability of a future deep overturn.

1. Introduction

The European pre-alpine and alpine regions are characterized by the presence of many deep and large lakes, which are distinctive landmarks, fundamental drinking water and economic resources, as well as major tourist attractions. A peculiar hydrodynamic feature of these basins is that a large amount of their deep water remains isolated during most of the year and can mix with the surface and oxygenated water only at the end of winter, when the thermal stratification weakens (Wetzel, 2001). Deep mixing events are a decisive factor for the evolution of water quality and biocenosis in lakes because they allow dissolved substances, such as oxygen and nutrients, to be distributed over the entire water body (Boehrer & Schultze, 2008). The extent of deep circulation is the outcome of the competition between density stratification and the active drivers of mixing. When stratification prevails, a prolonged isolation of deeper waters may result in hypolimnetic anoxic conditions, which are unsuitable for fish and zooplankton (North et al., 2014) and for human utilization (Robertson & Imberger, 1994; Schindler & Vallentyne, 2008). Moreover, the segregation of nutrients in the monimolimnion causes an epilimnetic nutrient depletion with consequences on the entire food web (North et al., 2014; O'Reilly et al., 2003; Verburg & Hecky, 2009; Yankova et al., 2017). When stratification weakens under the action of penetrative convection by surface cooling, density-driven plumes, wind-driven advection of turbulent kinetic energy and deep upwelling following wind stress (Bouffard & Wüest, 2019), lakes can experience a progressive erosion of their stratification which contributes to a more uniform spread of nutrients and oxygen and that can culminate in a lake turnover, evoking the idea of upwelling of bottom layers. The dynamics of wintertime deep-water renewal, traditionally considered mainly driven by vertical convective cooling, is instead highly three-dimensional (Biemond et al., 2021; Lemmin, 2020; Peng et al., 2024). Numerical and experimental studies developed in deep basins such as Lake Garda (Biemond et al., 2021), Rappbode reservoir (Bocaniov et al., 2014) and Lake Tahoe (Schladow et al., 2004), provided evidence of deep mixing events triggered by wind-driven upwelling. During these events, the free surface tilt that follows strong winds associated with weak stratification, determines a counter-directed slope of the isopycnals in the stratified meta and hypolimnion, which may rise at the upwind end and bring the bottom waters up to the surface ("full upwelling"), facilitating their mixing with the epilimnion (Monismith, 1986).

According to the projections of future lake-mixing regime worldwide, developed through numerical modeling (Butcher et al., 2015; Kraemer et al., 2015; Wahl & Peeters, 2014; Woolway et al., 2020; Woolway &

Merchant, 2019), thermal stratification strength and duration are expected to increase under global warming and mixing to become less frequent. According to Woolway and Merchant (2019), 25 ± 5% of altered lakes under the RCP 6.0 scenario with higher emissions are projected to change their mixing regime from monomictic to meromictic, becoming permanently stratified by the end of the century. Considering the ecological implications that could follow, including increased risk of hypoxic conditions, cyanobacterial blooms and thermal stress of fishes (Butcher et al., 2015), this scenario compels research work on overturns of deep lakes. The response of lake surface water temperatures to climate change is indeed well documented by data, while the understanding of the way these surface trends are translated into the more complex deep conditions is deficient. This is due both to limited subsurface observations (Anderson et al., 2021) and to the complexity of the driving physical processes (Ghane & Boegman, 2021). In this context, the studies that have investigated the role of chemical stratification in deep mixing are mostly limited to meromictic lakes, such as small pit lakes (Pieters & Lawrence, 2014; Schultze et al., 2017) and large tropical lakes (Katsev et al., 2017).

Using long-term temperature data from 26 lakes around the world, Kraemer et al. (2015) have shown that deep lakes have experienced the largest changes in lake stratification. Deep lakes south of the Italian Alps confirm reduced mixing depths and oxygen depletion in response to a reinforcement of their thermal stratification (Rogora et al., 2018). In some cases like Lake Idro, Lugano and Iseo, the effects are exacerbated by chemical stratification (Aeschbach-Hertig et al., 2007). Lake Iseo has shifted from monomictic to meromictic, experiencing deep anoxia in the last decades (Rogora et al., 2018) and accumulation of phosphorus, which is delivered to the lake by the main inflows and by the residual load from combined sewer overflows (Pilotti et al., 2021). Lau et al. (2020) showed that phosphorus, after settling from the upper layers, is also released as internal load by the sediments. Although the hypothesis that chemical stratification could have a role in the expected meromictic behavior of this lake is not new (Ambrosetti & Barbanti, 2005; Brizzio et al., 1999), so far this was unsupported by a carefully calibrated density equation for the deep layers of the lake, as well as by the analysis of high-resolution wind and temperature data, that exert a fundamental role on the overall resistance to mixing (Imberger & Patterson, 1990).

To overcome these limitations, we (a) developed a field campaign and applied the algorithm proposed by Boehrer et al. (2010) to assess the role of the ionic composition on the lake chemical stratification. This made it possible to quantify the role of the calcium carbonate precipitation, strictly connected to the trophic status of the lake, and of the sulfates, naturally present in the basin. The measured data were used to calibrate a site-specific equation that relates water density to temperature and electrical conductivity, following the algorithm proposed by Moreira et al. (2016). This approach has been successfully applied in several lakes (Boehrer et al., 2016; Ficker et al., 2019; Xu et al., 2022) and the obtained site-specific equation enables an easy computation of density based on the CTD (conductivity, temperature and depth) profiles, which are ordinarily measured in lakes. Moreover, we (b) made use of 9 years of high-resolution temperature and wind data, measured by a station moored on the lake surface, to quantify the role of stratification in resisting deep upwelling each year. The overall data set was finally analyzed (c) to provide a statistical interpretation of the effect of the chemical stratification and deep warming on the probability of deep-water renewal by wind-driven upwelling.

We believe that this comprehensive approach, that goes beyond the simple direct role of epilimnetic stabilization also to include the effect of hypolimnetic mineralization and the conflicting effect of deep warming, is general and can be used to shed light on the complex factors that lead to the modification of the stratification and on the extent of water renewal in other deep lakes.

2. Methods

2.1. Field Site

Lake Iseo is a large and deep Italian subalpine lake, with an area of 61 km^2, a volume of about 8 km^3 and a maximum depth of 256 m. The Oglio river (I1) and Italsider channel (I2), are the two main tributaries with an overall average annual inflow of 55 m^3/s.

The first detailed scientific analysis of Lake Iseo dates back to two field campaigns in May and November 1967 (Bonomi & Gerletti, 1967) and documents a monomictic lake, characterized by deep water at 250 m with 70% oxygen saturation and temperature $T = 5.75$°C. The average oxygen consumption in the layer between 100 and 200 m depth was 0.6 mg/L/year. Interestingly, a high oxygen content of bottom water is also documented in a previous qualitative survey of the lake (Monti, 1929). However, since the second half of the

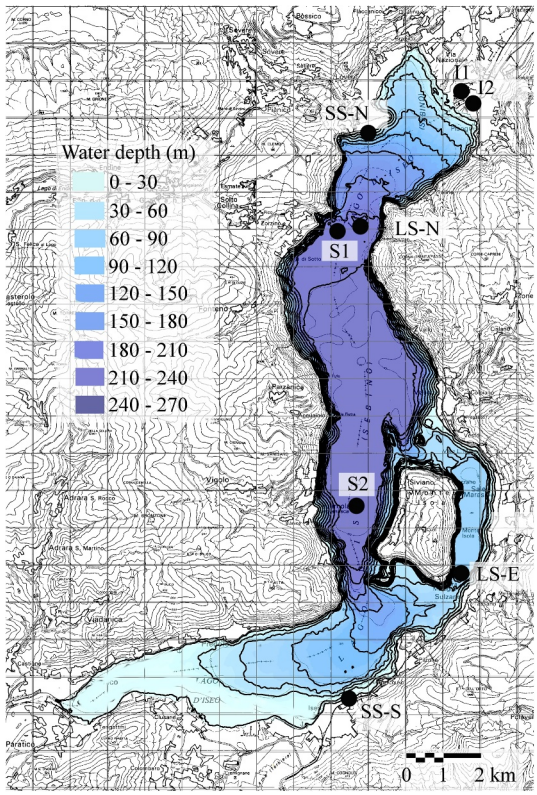

Figure 1. Bathymetry of Lake Iseo with isodepth lines at 30-m spacing, showing the location of the two main inflows (I1, I2), the sampling points (S1, S2), the lake stations equipped with thermistor chains (LS-N, LS-E) and the meteorological shore stations (SS-N, SS-S).

1980s the deep-water recirculation has been insufficient, except for two deep circulations in 2005 and 2006. During the periods of uncomplete mixing, deep water had gradually warmed with rates that could be estimated approximately ~0.05°C/year in the 2 decades 1985–1995 and 2007–2016, according to the temperature data reported by Garibaldi et al. (1995) and Rogora et al. (2018). At the same time, the waters below 100 m underwent a dramatic quality deterioration in term of oxygen and phosphorous concentrations (Rogora et al., 2018). At present, the monimolimnion retains 45% of the lake waters in anoxic conditions with 76% of the lake phosphorous. Considering that a similar situation is present also in the neighboring Lake Lugano and Lake Idro (Brizzio et al., 1999), Ambrosetti and Barbanti (2005) argued that it was favored by a permanent chemical stratification of the lake's waters. Whereas the peculiar presence of sulfate is due to the anhydrite present in the watershed (Garibaldi et al., 1995), the role of calcium and bicarbonate is connected to the precipitation of calcium carbonate in the epilimnion, due to the increase of waters pH during strong photosynthetic activity (Many et al., 2024), as documented in other lakes (e.g., Camacho et al., 2017). Recently, Valerio et al. (2019) provided experimental evidence that the density gradient at the interface between the mixolimnion and the monimolimnion of Lake Iseo can support large wind-driven internal wave motions. In wintertime, a tilt of ~20 m was observed at the interface's depth.

2.2. Field Data

We have managed a floating station in Lake Iseo since 2014, moored at a point where the lake is about 220 m deep. The station (see LS-N, Figure 1) was equipped with 12 thermistors down to a depth of 156 m from May-2014 to May-2017 and down to 97 m afterward (Pilotti et al., 2013). Water temperature has been monitored continuously with sampling frequency of 1/60 Hz and with ±0.01°C accuracy. Temperature was also measured with a similar instrument at LS-E (see Figure 1) at 12 different depths down to 50 m from June-2014 to June-2018; these measurements were used from February to March 2017 to replace missing LS-N's data. Meteorological forcings have been monitored by several stations in the lake's area. To the purpose of the presented analysis, we made use of the 1/60 Hz time series of wind speed and direction which we have measured since 2014 above the lake surface at LS-N, and since 2010 in proximity to the shore at SS-N and SS-S (details in Pilotti et al., 2013). Since May 2014 we have collected 8.7 years of temperature and wind data. Maintenance and occasional damages of the equipment implied 1.8 years of data gaps.

Vertical profiles of temperature, conductivity and oxygen were measured with 0.1 m vertical resolution during sparse field campaigns with a CTD probe (RINKO CTD profiler, by JFL Advantech Co.). Monthly values of these parameters are also made available at 6 references depths in the deepest basin (S2) by the Regional Agency for Environmental Protection (ARPA).

2.3. Water Density

In order to derive an equation of state for density in the mixolimnion and the monimolimnion of Lake Iseo, we made use of the ions concentration of two samples collected on 13 July 2018 at S1 (45.778°N, 10.055°E, see Figure 1) at the depth of 40 and 200 m and of a temperature, conductivity and oxygen profile measured at the same location with the CTD probe. We first applied the algorithm RHO-MV (Boehrer et al., 2010), with a second order approximation for temperature dependence and ionic strength based on the chemical composition obtained from the laboratory analysis of water samples. The RHO-MV approach has been tested for seawater composition against the UNESCO equation and the relative accuracy on freshwater density estimation resulted better than $1.5\ 10^{-5}$ according to Boehrer et al. (2010). We then followed the approach by Moreira et al. (2016) to calibrate a mathematical formula that relates density to temperature and electrical conductivity. This approach is based on the RHO-LAMBDA algorithm, whose application provided the density contribution of salts with an accuracy of 10% or better over a wide range of concentrations (Moreira et al., 2016).

After the density equation was calibrated, it was possible to compute the hourly time series of the density profiles for 9 winters (01st January–31st March) between 2015 and 2024 (2015–2021, 2023–2024, excluding 2022 when the thermistor chain was out of order) from the temperature and conductivity data available in the lake. Considering that the variation of conductivity profiles is rather limited in time (see details in Section 3.3), each year we assumed that the vertical conductivity profiles measured with the CTD probe and by ARPA at the end of winter were constant in the period January–March. The conductivity data measured at each temperature T (EC_T) were normalized at $T_{ref} = 25°C$ according to Boehrer and Schultze (2008) as:

$$EC_{Tref} = \frac{EC_T}{\alpha(T - T_{ref}) + 1} \quad (1)$$

assuming $\alpha = 0.02°K^{-1}$. Hourly averaged vertical temperature profiles were obtained by interpolating over the depths the time series measured by the thermistor chain between 0 and 97 m. In the monimolimnion, apart from short term fluctuations caused by internal waves, the temporal variation of temperature between January and March is usually less than 0.02°C. Accordingly, during each winter period, deep temperature values were assigned according to the profile measured at the end of that winter.

2.4. Lake Stability

The wintertime profiles were analyzed in terms of Schmidt stability, that is, by computing the work required to mix the entire water body to a uniform density in adiabatic conditions. We adopted Idso's methodology (Idso, 1973), that gives the mixing energy requirement S_t [J/m^2] per unit area:

$$S_t = \frac{g}{A_0}\int_0^H (z - z_V)\,A(z)\rho(z)\,dz \quad (2)$$

where g (m/s^2) is the acceleration due to gravity, H (m) is the maximum water depth, z_V (m) and $A(z)$ (m^2) are the center of volume and the area of the lake as a function of depth z, $\rho(z)$ (kg/m^3) is the depth-dependent density and A_0 (m^2) is the surface area of the lake. The analysis of stability was developed for 9 years using the data measured from 01st January to 31st March, when in Lake Iseo the weakening of thermal stability favors deep mixing. In this period, the chemical stratification plays a major role and the water column may thus be approximated by a two-layer system, with an interface at a the pycnocline depth z_T separating the mixolimnion and the monimolimnion, oscillating with a dominant V1H1 mode (Valerio et al., 2019).

The Schmidt stability expresses the resistance to mixing only, independently from the amount of energy supplied by wind to mix the system. Accordingly, the actual stability can be better expressed by the dimensionless Lake Number L_N (−) (Imberger & Patterson, 1990), that is, by the ratio between the stabilizing momentum supplied by the vertical stratification and the overturning momentum exerted by the water shear velocity u_* (m/s) driven by the wind at the lake's surface:

$$L_N = \frac{S_t\left(1 - \frac{z_T}{H}\right)}{\rho_0 u_*^2 {A_0}^{1/2}\left(1 - \frac{z_V}{H}\right)} \quad (3)$$

where ρ_0 is the water density at the surface. For $L_N > 1$, stratification is strong and dominates over the destabilizing wind action. Under these circumstances, the isopycnals are expected to be primarily horizontal. For $L_N < 1$, stratification is weak with respect to wind stress and the isopycnals are expected to experience strong seiching. Accordingly, L_N was used to identify the occurrence for deep upwelling in several deep lakes and reservoirs (Imberger & Patterson, 1990; Robertson & Imberger, 1994; Woolway & Merchant, 2019).

In this contribution, we computed the time series of L_N to estimate the probability of an upwelling of the monimolimnion during the observation period, highlighting the role of thermal and chemical stratification (see details in Section 3.4). Considering that the overturning momentum exerted by the shear velocity could be less effective with increasing depth, it is worthwhile noting that the proposed conceptualization provides a conservative criterion of upwelling when $L_N > 1$, while it could overestimate the occurrence of full mixing events in deep lakes.

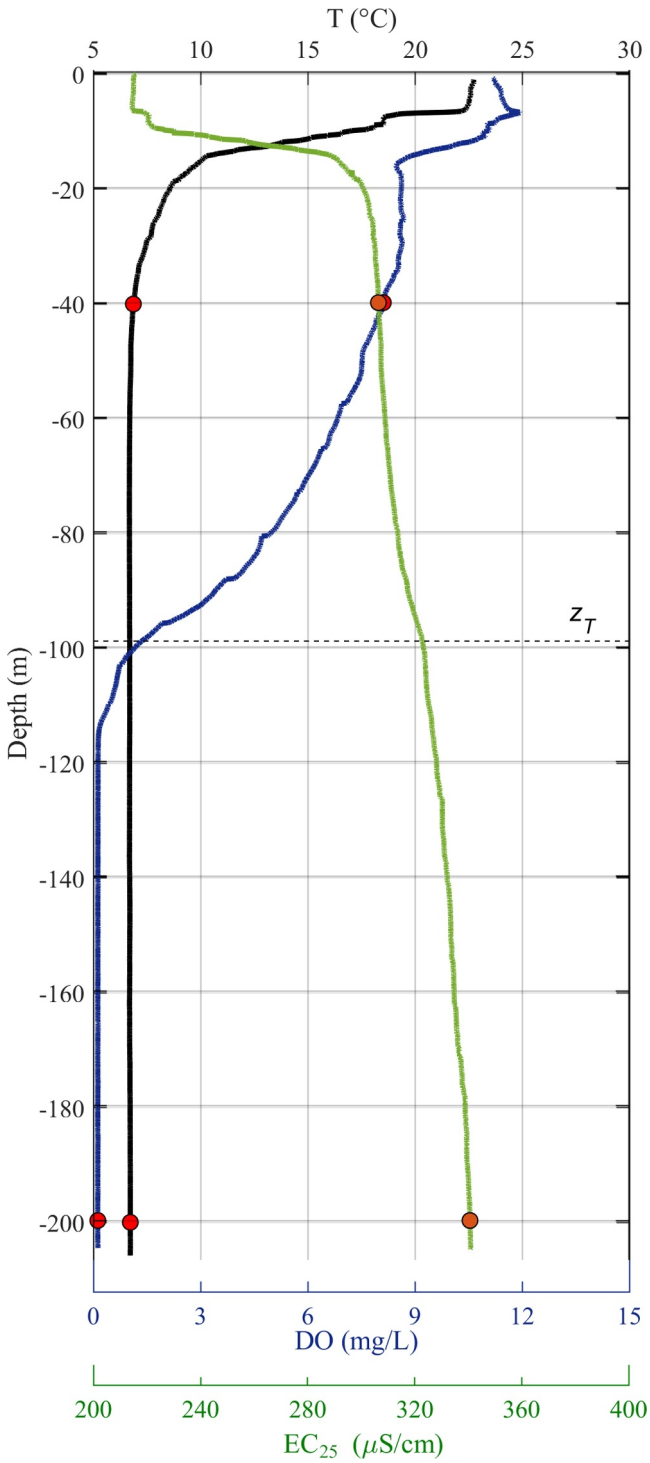

Figure 2. Vertical profiles of temperature T, dissolved oxygen DO and specific conductivity EC_{25} collected at S1 on 13 July 2018. The red dots mark the values in correspondence of the depth of the samplings, while the dashed line marks the chemocline location.

In wintertime, the oxygenated and uniform mixolimnion is distinctively separated from the anoxic and denser monimolimnion below. Accordingly, in the years when high-resolution profiles were available at end of winter, we located z_T in the region of larger gradients of density. Otherwise, we made use of the oxygen data in the following months to identify z_T as the depth where the oxygen concentration fell below 2 mg/L. The resulting z_T depths range between 70 and 110 m. To compute the time series of L_N, we made use of the hourly time series of the density profiles and of the wind speed measured at LS-N and SS-N. Here it is important to observe that, as shown by Valerio et al. (2017), a good representation of the internal wave field in Lake Iseo may be obtained by forcing the system with a uniform wind having the same power of the spatially varying one. Accordingly, we computed the hourly coefficients that minimize the difference between the power of the wind speed measured at a given location and the power of the spatially variable wind field, which was made available by the numerical simulations of Valerio et al. (2017). The time series of the local wind speed was thus corrected with these coefficients, making them more representative of the spatially varying wind field. For LS-N station, the coefficients range from 0.4 to 1.3, with an average equal to 0.8, because LS-N is located in an area where southerly winds are maximized. Following the theory of upwelling by Stevens and Imberger (1996), the setup time required to reach pseudo-steady-state conditions is one-quarter of the fundamental internal seiche period; accordingly, wind speeds and temperature profiles were also averaged over 18-hr periods, an interval which corresponds to one quarter of the average period of the main fundamental mode at the end of the stratified period (Valerio et al., 2019), when upwelling is likely to occur. To account for atmospheric instabilities, the shear velocity was computed with the algorithm provided by Verburg and Antenucci (2010), on the basis of air and water temperatures, relative humidity and atmospheric pressure measured by the LS-N and SS-N stations.

3. Results and Discussion

3.1. Determination of Density Based on the Composition of Solutes

The profiles collected in Lake Iseo highlight the presence of a permanent salinity stratification. Figure 2 shows the profiles of temperature, oxygen and conductivity measured at the sampling site in July 2018. The conductivity presents a large gradient of 0.6 $\mu Scm^{-1}m^{-1}$ between 90 and 100 m of depth, which marks the boundary between the mixolimnion and the monimolimnion. The ions concentration of the samples collected at 40 and 200 m was 240 and 265 mg/L, respectively. The concentration of each ion is shown in Table 1. Consistently, the conductivity normalized at 25°C increases from 306.3 to 340.4 μScm^{-1} between the two sampling depths.

We applied the algorithm RHO-MV (Boehrer et al., 2010) to calculate the density function of the two samples, obtaining the results shown in Table 2. It is possible to observe that at each temperature the density difference of the two samples is on average 25.00 mg/L, ranging between 24.42 at 30°C and 25.83 at 0°C.

It is important to analyze in detail the two density functions in correspondence of the winter temperatures (see Figure 3a). At 6.7°C, the water at 200 m is 1,000.157 g/L, while the water at 40 m reaches the same density at 6.05°C, due to its lower ionic content. Accordingly, in Lake Iseo a uniform temperature along the water column is not enough in itself to drive deep convective mixing. As long as the mixolimnion temperature is above 6.05°C, it

Table 1
Chemical and Physical Characterization of the Samplings Collected at S1 at 40 and 200 m of Depth on 13/07/2018

	z = 40 m	z = 200 m
Na^+ (mg/L)	3.5	3.5
K^+ (mg/L)	1.2	1.3
NH_4^+ (mg/L)	<0.05	0.22
Ca_2^+ (mg/L)	42.7	49
Mg_2^+ (mg/L)	10.1	11.2
Mn_2^+ (mg/L)	<0.005	0.241
Fe_2^+ (mg/L)	<0.02	0.027
Al_3^+ (mg/L)	<0.02	<0.02
Cl^- (mg/L)	3	3
F^- (mg/L)	0.2	0.2
NO_3^- (mg/L)	4	<1
HCO_3^- (mg/L)	127	142
CO_3^{2-} (mg/L)	<5	<5
SO_4^{2-} (mg/L)	48	54
H_4SiO_4 (mg/L)	3.8	6.9
DOC (mg/L)	0.8	0.8
pH (−)	7.9	7.6
T (°C)	6.86	6.72
EC_{25} (μScm^{-1})	306.26	340.39
DO (mg/L)	8.11	0.12

remains less dense than the underlying monimolimnion, and a further cooling is needed to reach a uniform density profile.

The RHO-MV methodology allows also to determine the contribution of each ion to the water density. Table 3 shows that the main contribution comes from calcium (Ca^{2+} 41.6%), bicarbonate (HCO_3^- 31.4%) and sulfate (SO_4^{2-} 18%). Even though the bicarbonate is the ion that presents the highest concentration increase, its contribution is lower than that of the calcium because of its lower density fraction, defined as the ratio between the solute and mixture's mass per unit volume ($\widetilde{\Delta\rho}(HCO_3^-) = 0.528$; $\widetilde{\Delta\rho}(Ca^{2+}) = 1.668$). For the same reason ($\widetilde{\Delta\rho}(SO_4^{2-}) = 0.761$), 6.3 mg/L of difference in the calcium concentration between 40 and 200 m implies 10.5 mg/L of density increase, while 6.0 mg/L of difference in the sulfate concentration implies only 4.6 mg/L of density difference.

3.2. Determination of Density Based on Conductivity

We calibrated a site-specific equation that relates density to temperature, T (°C), and conductivity normalized at 25°C, $EC_{25}(mS/cm)$, making use of the RHO-LAMBDA algorithm proposed by Moreira et al. (2016), where two specific coefficients are determined based on the composition of solutes. We repeated the procedure with reference to the chemical composition of the two samples, obtaining for the 40 m composition:

$$\rho_1(T, EC_{25}) = \rho(T) + EC_{25}(0.678 - 0.0015(T - 25)) \quad (4)$$

and for the 200 m composition:

$$\rho_2(T, EC_{25}) = \rho(T) + EC_{25}(0.683 - 0.0015(T - 25)) \quad (5)$$

The first term of the right side is the density of pure water and may be computed with the expression provided by Tanaka et al. (2001):

$$\rho(T) = \left[1 - \frac{(T + a_1)^2 (T + a_2)}{a_3 (T + a_4)}\right] \rho_{MAX} \quad (6)$$

where ρ_{MAX} = 999.975 g/L, $a_1 = -3.983$°C, a_2 = 301.797°C, a_3 = 522,528.9°C and a_4 = 69.349°C.

The difference in the obtained density profiles provided by the two equations is negligible (e.g., on July 2017 the relative differences were below 10^{-3}%), so that both may be indifferently used along the whole water column in Lake Iseo. We thus averaged the parameters, obtaining a single equation, with a considerable practical simplification:

$$\rho(T, EC_{25}) = \rho(T) + EC_{25}(0.681 - 0.0015(T - 25)) \quad (7)$$

Equation 7 provides density on the basis of measurements of temperature and electrical conductivity, easily obtainable by means of a CTD profiler. For the following consideration it is interesting to consider the sensitivity of this equation to temperature and conductivity, obtained by computing the normalized total differential of Equation 7:

Table 2
Temperature Dependence of Density in the Case of the Pure Water (ρ_{H2O}) and of the Water With the Ionic Composition Resulted From the Analysis of the Samples Collected in Lake Iseo at 40 m (ρ_1) and 200 m (ρ_2)

		40 m	200 m	
T (°C)	ρ_{H2O} (g/L)	ρ_1 (g/L)	ρ_2 (g/L)	$\Delta\rho_{12}$ (mg/L)
0	999.843	1,000.063	1,000.089	25.83
1	999.902	1,000.121	1,000.147	25.76
2	999.943	1,000.162	1,000.188	25.69
3	999.967	1,000.185	1,000.211	25.62
4	999.975	1,000.193	1,000.218	25.56
5	999.967	1,000.184	1,000.209	25.49
6	999.943	1,000.160	1,000.185	25.43
7	999.904	1,000.120	1,000.146	25.37
8	999.851	1,000.066	1,000.092	25.31
9	999.784	999.999	1,000.024	25.26
10	999.703	999.917	999.942	25.20
11	999.608	999.822	999.847	25.14
12	999.500	999.713	999.739	25.09
13	999.380	999.593	999.618	25.04
14	999.247	999.459	999.484	24.99
15	999.103	999.314	999.339	24.94
16	998.946	999.157	999.182	24.90
17	998.778	998.988	999.013	24.85
18	998.598	998.809	998.833	24.81
19	998.408	998.618	998.642	24.77
20	998.207	998.416	998.441	24.73
21	997.995	998.204	998.229	24.69
22	997.773	997.982	998.006	24.65
23	997.541	997.749	997.774	24.62
24	997.299	997.507	997.531	24.58
25	997.047	997.255	997.279	24.55
26	996.786	996.993	997.018	24.52
27	996.515	996.722	996.747	24.49
28	996.235	996.442	996.466	24.47
29	995.946	996.153	996.177	24.44
30	995.649	995.855	995.879	24.42

Note. The last column reports the density difference between ρ_1 and ρ_2 in correspondence of each temperature.

$$\begin{cases} \dfrac{d\rho}{\rho} = A\dfrac{dT}{T} + B\dfrac{d\mathrm{EC}_{25}}{EC_{25}} \\ A = \dfrac{T}{\rho}\dfrac{\partial\rho}{\partial T} \\ B = \dfrac{\mathrm{EC}_{25}}{\rho}\dfrac{\partial\rho}{\partial \mathrm{EC}_{25}} \end{cases} \quad (8)$$

The partial derivatives $\frac{\partial\rho}{\partial T}$ and $\frac{\partial\rho}{\partial \mathrm{EC}_{25}}$ can be computed analytically from Equations 6 and 7 and expressed as functions of temperature and conductivity. The A/B ratio (where in our case A is negative for $T > 4°\mathrm{C}$) gives the ratio between the density variation induced by the same percentage change of temperature and of conductivity. Considering a set of EC_{25} values typical of Lake Iseo (0.2–0.4 mS/cm), A, B and A/B can be represented as family of curves, having EC_{25} as parameter. The A/B iso lines are shown in Figure 3b as a function of T and EC_{25}. For instance, when $T = 6.7°\mathrm{C}$ and $\mathrm{EC}_{25} = 0.3\ \mathrm{mS/cm}$, $A/B = -1.326$, showing that the decrease of density with temperature is dominant with respect to the density increase caused by the same percentual change of conductivity.

3.3. Analysis of the Density Profiles in Lake Iseo

In Lake Iseo, since 2010 the water below 150 m did not experience any mixing with the overlying water. The absence of deep oxygenation documented by Rogora et al. (2018) until 2016 has continued in the following years, as shown by the oxygen profiles shown in Figure 4e. With deeply penetrative mixing being suppressed, hypolimnion is expected to warm (Livingstone, 1997), at a rate which can be quantified since 2014, when we started high resolution measurements of deep temperature (see Figure 4). In the period 2014–2016 the temperature was continuously measured at 97 and 156 m of depth, observing similar rate of increase (0.107 and 0.090°C/year). In the following period temperature was measured at 97 m of depth, revealing an increase from 6.45 to 7.31°C in 10 years (0.086°C/year). During the warmest years, such as 2023, the warming rate was greater than 0.1°C/year. The CTD profiles collected in Lake Iseo since 2016 indicate a uniform warming trend of the deep waters, at an average rate of 0.062°C/year, which drove the deep layers from 6.56°C to 7.05°C in 8 years. Conversely, it is interesting to observe that conductivity below 120 m did not show any relevant temporal trend, with values deviating ±5 µS/cm around the mean, consistently with the observations in the neighboring Lake Lugano, where the increase of conductivity was only about 5 µS/cm from 1990 to 2001 in the lowermost 100 m (Aeschbach-Hertig et al., 2007).

At the end of the limnological winter, some temperature profiles show cold layers above warmer layers (see Figure 5). The application of Equation 7 provides an explanation to the occurrence of these thermal anomalies between the mixolimnion and the monimolimnion. The profiles of potential density in panel (c), which monotonically increases with depth in all the considered cases, demonstrate their stability. Figure 5 shows that on 8 February 2017, the gradient in conductivity between 60 and 80 m of depth prevents the convective circulation from penetrating deeper than 60 m. In the layers between 60 and 90 m the conductivity increases by 21 µS/cm, which, according to the calibrated density equation, corresponds to 14 mg/L of density difference at 6.7°C. Accordingly, 0.15°C of temperature difference across the chemocline, corresponding to 6.8 mg/L of density difference, does not trigger any instability and cannot drive a vertical convection. This would be instead possible in correspondence of a temperature difference of 0.35°C, that would require a much stronger cooling of the water layer above. A similar situation

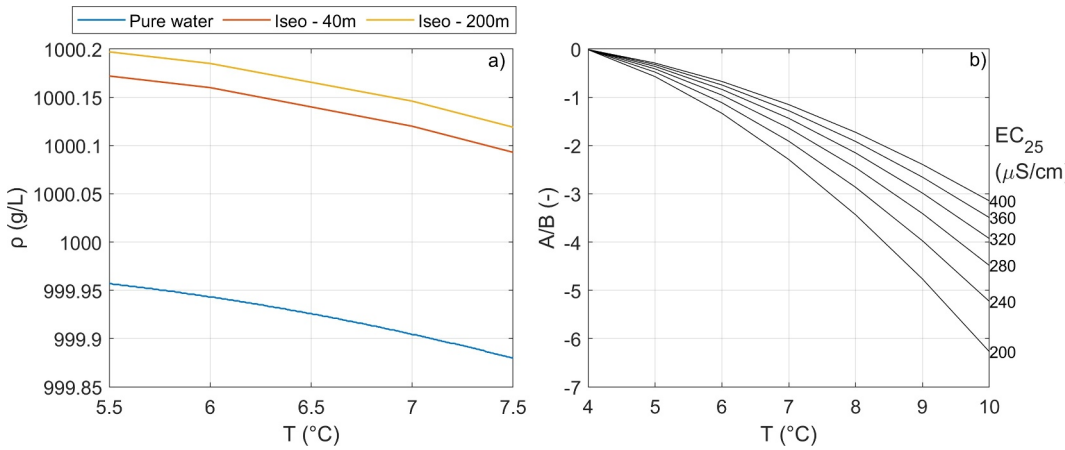

Figure 3. (a) Density of pure water and of the water with the ionic composition of the samples collected in Lake Iseo at 40 and 200 m between 5.5 and 7.5°C. (b) Sensitivity of density to temperature and conductivity normalized at 25°C, expressed with the ratio between the quantities A and B defined in Equation 8.

can be observed on 8 March 2018 at the depth of 70 m, where the water is slightly colder than that of the monimolimnion (6.66°C vs. 6.68°C). The presence of the salinity stratification inhibits the potential of this layer to penetrate and renew the deep waters. In the profiles it is also possible to observe more confined layers with strong gradients in temperature, which are likely caused by the I1 and I2 inflows intrusion, which are documented for this lake (Pilotti et al., 2018).

Table 3
Contribution of the Single Ions to the Density Difference Δρ Between 40 and 200 m

	Δρ (mg/L)
H^+	0
Na^+	0
K^+	0.089
NH_4^+	0.056
Ca^{2+}	10.508
Mg^{2+}	2.462
Mn^{2+}	0.357
Fe^{2+}	0
Fe^{3+}	0
Al^{3+}	0
OH^-	−0.007
Cl^-	0
F^-	0
NO_3^-	−1.842
HCO_3^-	7.926
CO_3^{2-}	0
SO_4^{2-}	4.565
H_4SiO_4	1.122
Sum	25.24

3.4. Interannual Variability of Deep-Water Renewal Driven by Upwelling

3.4.1. Role of Chemical Statification

To study the role played by chemical stratification on the stability, we expressed the density profile $\rho(z)$ as the sum of two contributions: $\rho_{ml}(z) = \rho(T(z), EC_{25ml})$, computed as a function of the temperature profile and of the average conductivity which characterizes the upper well mixed 50 m layer and the additional density $\Delta\rho_{ml}(z) = \rho(T(z), EC_{25}(z)) - \rho(T(z), EC_{25ml})$ associated to the local difference in the conductivity. Accordingly, considering the linearity of Equation 2 with respect to density, the stability can be decomposed in two contributions, S_t^T and S_t^C, which mostly reflect the role of thermal and chemical stratification, respectively:

$$S_t = \frac{g}{A_0}\int_0^H (z - z_V)\, A(z)\rho_{ml}(z)\, dz + \frac{g}{A_0}\int_0^H (z - z_V)\, A(z)\Delta\rho_{ml}(z)\, dz = S_t^T + S_t^C \quad (9)$$

The upper panel of Figure 6 shows the time series of the L_N of Lake Iseo during the investigated period, obtained by processing the measured wind speed as explained in the Methods and using the overall stability S_t. The minimum L_N values occurred between the beginning of February to the first half of March and were always above the threshold $L_N = 1$, consistently with the evidence of a mixing depth always above the chemocline's depth. In the lower panel of Figure 6 we compare more in detail the time series of L_N for a cold (2019) and a warm (2024) winter; the computation was repeated also using the thermal stability S_t^T only, simulating a situation without the

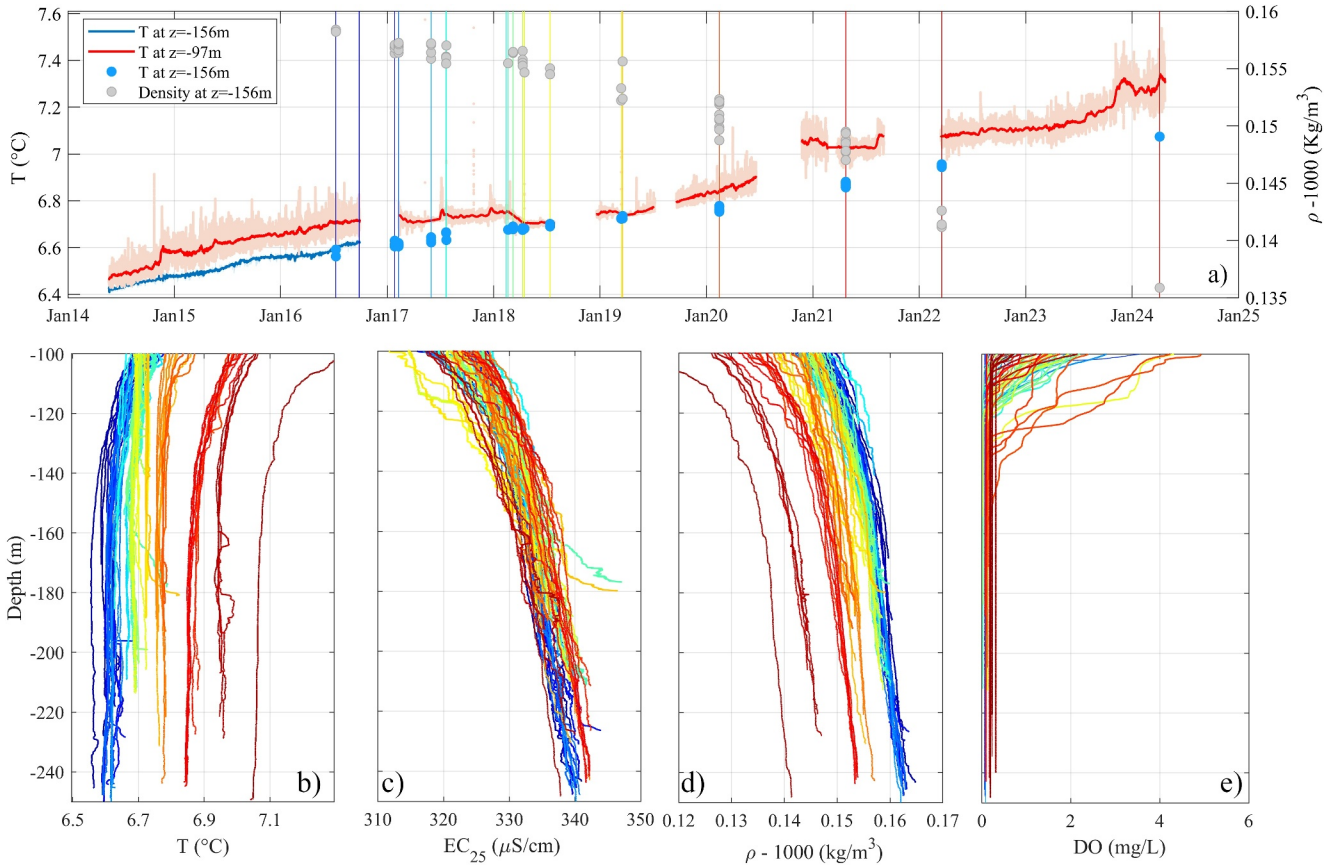

Figure 4. Trend of (a) deep temperature and density in Lake Iseo in the last 10 years and deep vertical profiles of (b) temperature, (c) conductivity, (d) density and (e) dissolved oxygen. A vertical line having the same color of each profile (b–e) is added in panel (a) to show when the profile was measured.

stabilizing effect of the chemical stratification. Whereas in 2024 the L_N values remained above the threshold, providing evidence that the thermal stratification alone was able to inhibit deep mixing, our data show that in 2019 L_N would have dropped below 1 for a week in February. Accordingly, it is likely that a full upwelling would have occurred in winter 2019 without the stabilizing effect of the chemical stratification. The same effect was observed for a shorter period of time on February 2017 and March 2018.

A synthesis of the computed results for the 2015–2024 winter period can be obtained by considering the relative frequency of occurrence of the S_t and L_N values (see Figure 7). The chemical stability S_t^C does not show significant variations among years, ranging from 864 to 1,103 Jm^{-2} and justifying the shift between the frequency distribution of the total and thermal winter stability reported in Figure 7a. Because of the chemical stratification, the total stability is always larger than 821 Jm^{-2}, suggesting a strong stabilization operated by the dissolved substances. To correctly quantify the actual stabilizing effect in relation to the destabilizing forces, Figure 7b shows the frequency distribution of the L_N, computed with and without accounting for the chemical stratification in the expression of the stability. The comparison between the curves shows a general reduction in the winter mixing, with an increased occurrence of $1 < L_N < 10$ from 4.5% to 27% in the observations. Interestingly, the relative frequency of $L_N < 1$, corresponding to the condition of full upwelling occurrence, is 0 in the present condition, while it would be 3.3% if the chemical stratification were neglected.

3.4.2. Role of Wind

To provide a more tangible way to look at the stabilizing effect of the chemical stratification, we quantified the increase in friction velocity that should occur to counteract the increase in stability in the deeper waters, based on the definition of Lake Number. An upwelling and consequent mixing of the monimolimnion should occur in correspondence of a wind event that causes $L_N < 1$ for a period longer than a quarter of the main internal wave

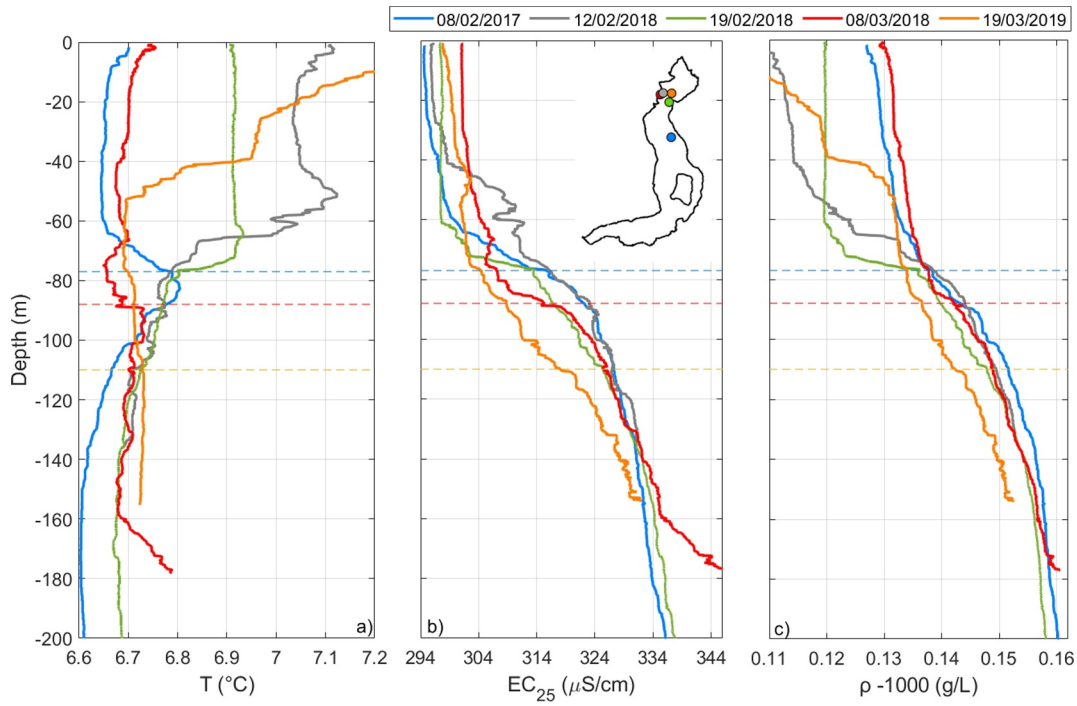

Figure 5. Vertical profiles of (a) temperature T and (b) conductivity EC_{25} measured in winter 2017, 2018 and 2019 at the locations marked in panel (b). In panel (c) the potential density profiles computed by Equation 7 are shown. The dashed lines mark the top of the monimolimnion at the end of winter 2017, 2018 and 2019.

mode (Stevens & Imberger, 1996). Accordingly, Equation 3 provides the space and time averaged critical shear velocity threshold u_*^{cr} as:

$$u_*^{cr} = \sqrt{\frac{\left(S_t^T + S_t^C\right)\left(1 - \frac{z_T}{H}\right)}{\rho_0 A_0^{\frac{1}{2}}\left(1 - \frac{z_V}{H}\right)}} = \sqrt{1.48 \cdot 10^{-7}\left(S_t^T + S_t^C\right)} \tag{10}$$

Figure 8a shows the shear velocity threshold as a function of the thermal stability S_t^T, comparing the relationship in the current situation, characterized by the presence of a chemical stratification ($S_t^C = 1{,}037\ \mathrm{Jm}^{-2}$), and in the theoretical case of a chemically uniform condition ($S_t^C = 0\ \mathrm{Jm}^{-2}$), when only thermal stratification matters. The curves indicate the minimum shear velocity needed to induce upwelling in correspondence of a given thermal stratification. Note that in presence of chemical stratification, the thermal stability S_t^T can enter the range of negative values, physically corresponding to water layers below z_V that are warmer than the layers above. This situation would be unstable without a chemical stratification.

Making use of the overall time series of wind speed measured at the floating station in the winter period, averaged over time and space as previously explained, it is possible to associate each shear velocity values with an exceedance probability p, defined for each value as the ratio between the number of times the value is exceeded divided by the number of observations. Accordingly, it is possible to associate a probability of upwelling p when a given thermal stratification is present in the lake, and this is done in Figure 8b with and without chemical stratification.

When the lake reaches minimum values of thermal stability each winter, the probability that an overturn by upwelling would occur depends on the probability that the shear velocity overcomes the threshold indicated by the curves shown in Figure 8b. Assuming each winter day from January to March as an independent occasion for the wind to overcome a fixed threshold, the computed values allowed us to estimate the probability P of lake overturn driven by upwelling. For each winter, the curve in Figure 8b can be used to associate n probability values p_i of wind threshold exceedance to the daily time series of n measured thermal stabilities. Based on the theory of independent repeating events, the overall probability P of lake overturn can be computed as the probability that

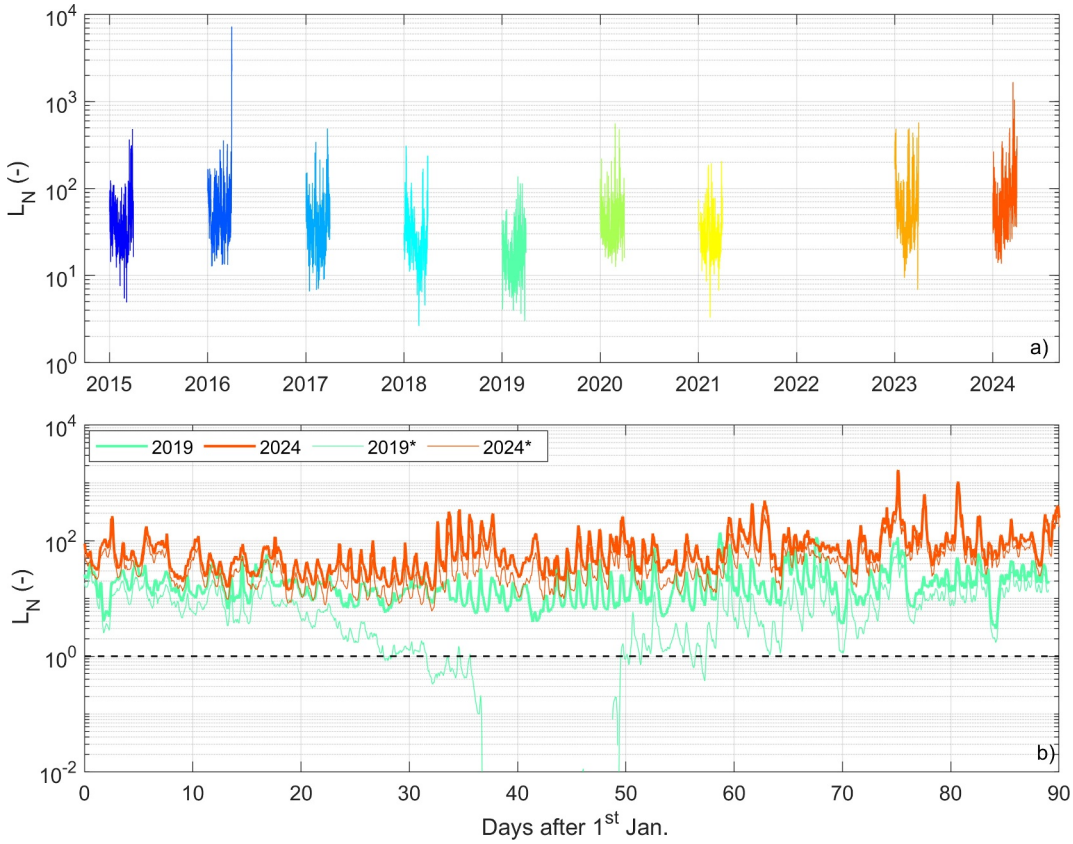

Figure 6. (a) Time series of L_N of the lake during the 9 winters (01st January–31st March) between 2015 and 2024. (b) Comparison between the 2019 and 2024 time series, obtained from Equation 3 with (thick line) and without (thin line) accounting for the chemical stratification in the stability of the water column. The dashed line marks the theoretical threshold for the monimolimnion upwelling ($L_N < 1$). The vertical axis is limited between 10^{-2} and 10^4: in the days 37–49, the 2019* line reaches values lower than 10^{-2}.

the wind overcomes the threshold at least once in a winter, which is the complementary of the probability that the wind never exceeds the threshold:

$$P = 1 - \prod_{i=1}^{n} (1 - p_i) \tag{11}$$

Consistently with the results obtained in 3.4.1, the probability P of lake full upwelling is zero for the whole time series. Conversely, considering the case of a chemically uniform water column, we obtained $P > 0$ in 2017 (98%), 2018 and 2019 (100%) and 2021 (1%), confirming that from 2017 to 2019 deep mixing was inhibited by the chemical stratification.

Considering an ordinary winter-time thermal stability of 100 Jm^{-2}, in absence of chemical stratification the threshold of the shear velocity u_*^{cr} is 0.004 m/s, an event with a 16% probability of exceedance, according to the observed wind series. This high probability of exceedance of the wind threshold could characterize the situation of Lake Iseo in absence of anthropic pressure and is consistent with the monomictic behavior attested by the first samplings in 1967 (Bonomi & Gerletti, 1967). In correspondence of the same value of thermal stability (100 Jm^{-2}), the chemical stratification led to an increase of the critical shear velocity u_*^{cr} from 0.004 to 0.013 m/s. Assuming a drag coefficient equal to 0.0013, this latter threshold would correspond to an average wind speed over the lake's surface higher than 10.4 m/s for more than 18 hr, representing an exceptionally strong storm for this lake. In the observation period, the measured winds, scaled in space and averaged over 18 hr, had a mean speed of 2.4 ± 0.6 m/s and never exceeded 6.5 m/s.

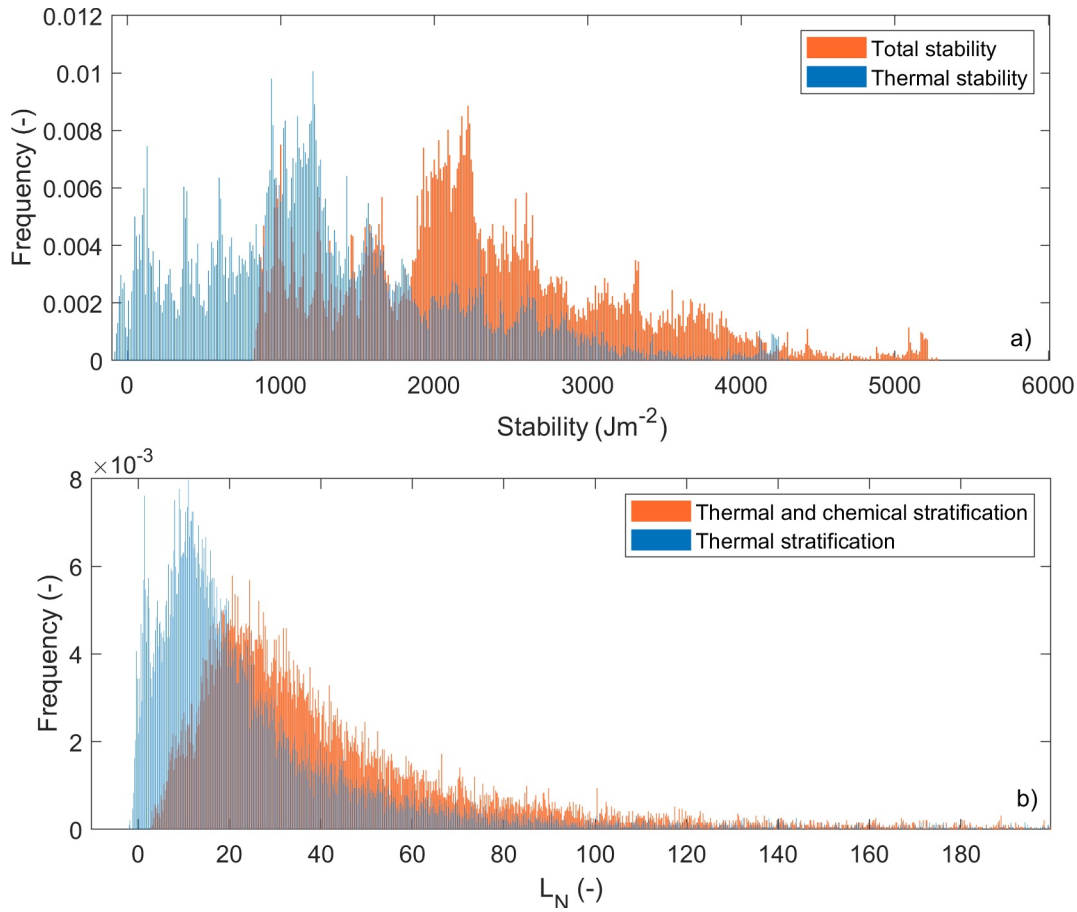

Figure 7. (a) Frequency of occurrence of S_t, S_t^T and (b) of L_N, computed with the 18-hr running-averaged wind and thermal stratification for 9 winters. Panel (b) compares the distribution of L_N, obtained with (orange line) and without (blue line) accounting for the chemical stratification of the water column. The x-axis was limited to 200.

Accordingly, overturns with the current chemical stratification could be possible in case of increased maximum wind speeds. We thus tried to test the effect of modified wind speeds on the probability of deep mixing, keeping the same thermal condition of the water column. In Figure 8b, for example, the dashed lines show the increased

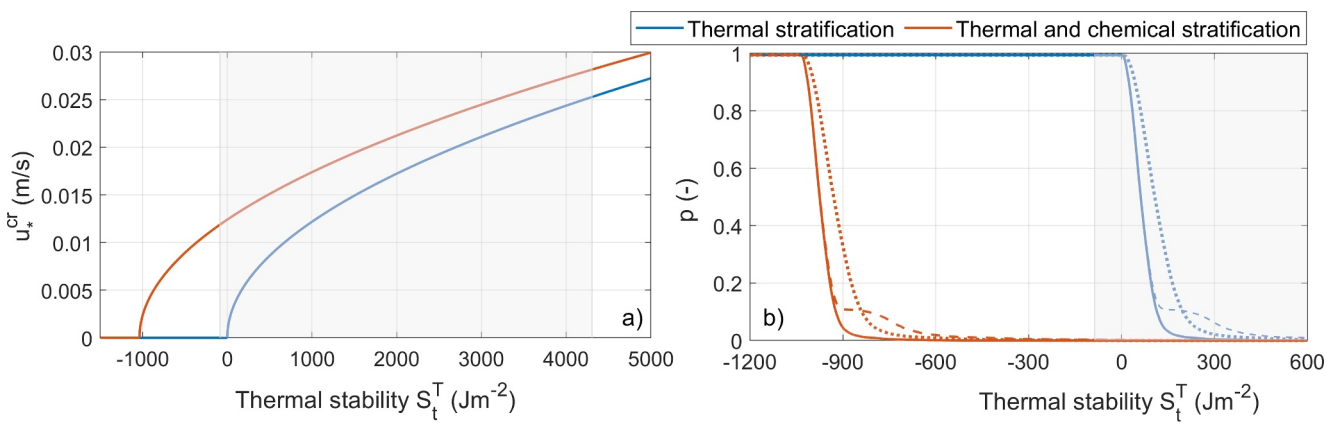

Figure 8. (a) Shear velocity threshold, u_*^{cr}, corresponding to the condition $L_N = 1$ as a function of the thermal stability S_t^T of the water column. (b) Probability of upwelling occurrence for a given value of thermal stability. The dotted line refers to a uniform 30% of increase of the lake's average wind, while the dashed one refers to a 50% of increase of the wind values above the 90th percentile only. In both panels, the red and blue lines make reference to the situation with and without chemical stratification; the shaded areas mark the range of thermal stability measured during the observation period.

probability of full upwelling for a 50% increase of wind speeds higher than the 90th percentile, spatially averaged on the lake. Despite the very significant increase in wind, the upwelling probability increases only slightly, becoming higher than zero in correspondence of the thermal conditions observed in 2017 (P = 3%), 2018 (P = 2%), 2019 (P = 5%) and 2021 (P = 0.1%). A similar result is obtained by a general 30% increase of the wind speeds (see dotted lines in Figure 8b).

The obtained results emphasize the importance of including the expected changes in the extreme values of the wind field in the analysis of the effects of climate change on lakes stability. However, while there is consensus that climate change will imply an increase in average temperature, at present, in spite of the recent exceptional Vaia storm (e.g., Rainato et al., 2021), there is no evidence of considerable modification of the wind field in the alpine area (Gobiet et al., 2014). Accordingly, it is still challenging to predict the extent of variations of the extreme winds at the local scale, both in strength and duration. However, in the specific case under consideration, the potential effect of increased wind speeds appears poorly effective in enhancing complete mixing in presence of the current chemical stratification, unless accompanied by cold meteorological conditions, sufficiently long to further reduce the thermal stratification.

3.4.3. Role of Deep Warming

Beside higher wind speeds, Figure 8b shows that deep mixing is also favored by reduced values of thermal stabilities. To conclude the analysis, it is thus important to consider the effects of deep warming on the thermal stability of the lake. This point is usually overlooked in the discussion regarding lake stability but actually deserves careful consideration, as originally observed by Livingstone (1997) who argued, on the basis of the analysis of deep temperature in several lakes, that deep warming could become a driver for complete mixing regardless of the degree of severity of the winter.

The winter profiles collected since 2016 indicate a uniform warming trend of the deep waters, at an average rate of 0.062°C/year, which drove the deep layers from 6.56°C to 7.05°C in 8 years. Considering Equation 8, there is evidence that the waters in the monimolimnion are becoming progressively lighter due to warming: the calibrated Equation 7 indicates a decrease in density of about 0.023 kg/m^3 in 8 years, due to the temperature increase, which implies a decrease of thermal stability of 755 J/m^2, which could partially compensate the stabilizing effect of the higher conductivity. The proposed analysis can be useful also to quantify the role of deep warming on the probability of a full upwelling, keeping all the other factors equal. To this purpose, for each year within the 2015–2024 period, we computed the time series of the L_N values repeating the same wind and thermal conditions observed between January and March, but applying a warming rate of 0.062°C/year in the monimolimnion. In this way, we obtained 9 time series of L_N values, where the thermal stability progressively decreased due to deep warming, until it fell below the stability threshold $L_N = 1$.

Considering 2019, that comprises the coldest winter in the investigated period, the minimum stability was observed on 11th February (822 J/m^2), when the averaged wind speed was 3.7 m/s, corresponding to a $L_N = 5.9$. With the addition of a deep warming trend, stability progressively decreased, and after 8 years and an overall deep warming of 0.5°C, stability reduced to 125 J/m^2 and L_N became lower than 1, indicating deep mixing by wind upwelling. In 2024, instead, corresponding to the warmest winter in the 2015–2024 period, a minimum L_N of about 13 happened on 2nd February, with an average wind speed of 3.2 m/s and a stability of 1,862 J/m^2. To counteract this stronger thermal stability, a much larger deep warming was needed and only after 15 years, with a deep temperature increase of 0.93°C, L_N became lower than 1.

One could observe that in these simulations we focused on deep warming only, disregarding the variations in surface temperatures. However, in real situations, climate change will affect both the surface layers temperature, with a stabilizing effect, and the deep layers, with a destabilizing one. In average terms, a constant rate of increase of air temperature raises the surface waters temperature with higher rates than deeper ones, resulting in the tendency of increased thermal stability in deep lakes (Woolway & Merchant, 2019). However, whereas the deep warming is characterized by a slow and steady increase, which integrates conditions across years, also under the effect of geothermal heat fluxes (Finckh, 1981), the upper waters undergo a more variable thermal dynamic, which is directly affected by short-term changes in weather conditions. It is thus not unlikely that in case of extreme events, which are expected to worsen due to climate change (Easterling et al., 2000), ordinary or even cold winters could occasionally lead to strong cooling of the surface layers.

Therefore, future winters with a warmer monimolimnion and an upper layer with the same temperature profile considered in the 2015–2024 period can reasonably be envisaged. Should this happen, the obtained results lead to the conclusion that the actual warming rates of the monimolimnion could induce a turnover of the lake even in ordinary winters, supporting the theory of "intermittent meromixis" speculated by Lau et al. (2020) in a climate change scenario.

4. Conclusions

A major concern of the scientific community working on deep lakes is the progressive enhanced isolation and consequent de-oxygenation of the deep waters that have been observed in the last decades. Recent studies speculate the aggravation of this situation in a climate-change scenario (Woolway & Merchant, 2019), but the time-dynamics and the effect of this evolution is still uncertain because of the insufficient knowledge of the factors controlling deep mixing in lakes (Ghane & Boegman, 2021) and the general lack of subsurface observations (Anderson et al., 2021), in contrast with the increased availability of surface data provided by satellite monitoring (Calamita et al., 2024).

In this study we investigated the insufficient mixing in Lake Iseo, a deep Italian lake, trying to understand whether it has been an effect of the direct anthropogenic pollution or of the changing climate conditions, and whether the deep-water renewal will in future be replaced more by sporadic and partial deep water formation events rather than full overturns.

The analysis of the chemical composition of the Lake Iseo waters highlighted 25.24 mg/L of permanent density difference between the epilimnion and the monimolimnion in this 256 m deep lake. We showed that 73% of this density difference is due to the gradient in calcium and carbonate. The analysis allowed us to provide a simple mathematical equation by which conductivity profiles, ordinarily measured using a CTD, can be used to estimate density stratification and stability. Combining this equation with 9 years, high-resolution wind and water temperature data, we quantified the resistance of Lake Iseo to deep upwelling in terms of Lake Number. In 3 out of 9 winters the chemical stratification inhibited a lake overturn; in the other cases, instead, deep mixing wouldn't have occurred, independently from the chemical stratification. Accordingly, the density increase due to mineralization (Boehrer et al., 2017) has played a fundamental role in the total blockade of this mechanism over the last decades, providing quantitative evidence of the role played by the anthropogenic pressure in the watershed (Pilotti et al., 2021) on the trajectory to meromixis of this deep lake.

According to our computations, it appears unlikely that variations of the wind field will be enough to counteract the stabilizing effect of mineralization. A more progressive and certain destabilizing effect could be provided by the hypolimnetic warming, which is occurring at an average rate of 0.062°C/year. The identified density equation shows that this process compensates for the stabilizing effect of dissolved substances in the deep layer. Accordingly, considering that occasionally cold winters will also be possible in a climate-change scenario, future mixing of the lake monimolimnion is not unlikely. The ecological relevance of these results suggests the need of a deeper understating of the different mixing processes in Lake Iseo. The proposed approach is based on a conceptualization of deep mixing, which accounts for upwelling only and is based on a simplified balance between the stabilizing momentum by stratification and the destabilizing momentum by wind. It could be improved by three-dimensional numerical simulations, which would shed light on all the complex sub-basin-scale processes involved in turnovers such as convective plumes from sidearms or secondary circulations (Ghane & Boegman, 2021).

In conclusion, it does not seem that chemically stratified deep lakes are necessarily doomed to meromixis, but more likely to periods of longer isolation alternated by sporadic overturns triggered by deep warming. After full circulation, the entire water column of these lakes would be homogenized, reaching low level of dissolved oxygen, which could threaten the whole aquatic ecosystem in the lake with asphyxiation, and feeding the euphotic zone with pulse phosphorous, which can trigger mass phytoplankton growth. These considerations provide further reasons to look with concern to the evolution of the mixing regime of the pre-alpine deep lakes, even in cases where a chemical gradient has reinforced their stability by surface warming.

Data Availability Statement

The experimental data measured in Lake Iseo and used in this study are freely available at this repository: https://hydraulics.unibs.it/hydraulics/dati-scaricabili/dati-scaricabili-wrr2025/.

Acknowledgments
We would like to thank Eng. Sergio Scattolini for his support in the calibration of the density equation. We also acknowledge ARPA for providing monthly conductivity data used in this paper. Open access publishing facilitated by Universita degli Studi di Brescia, as part of the Wiley - CRUI-CARE agreement.

References

Aeschbach-Hertig, W., Holzner, C. P., Hofer, M., Simona, M., Barbieri, A., & Kipfer, R. (2007). A time series of environmental tracer data from deep meromictic Lake Lugano, Switzerland. *Limnology & Oceanography*, *52*(1), 257–273. https://doi.org/10.4319/lo.2007.52.1.0257

Ambrosetti, W., & Barbanti, L. (2005). Evolution towards meromixis of Lake Iseo (Northern Italy) as revealed by its stability trend. *Journal of Limnology*, *64*(1), 1–11. https://doi.org/10.4081/jlimnol.2005.1

Anderson, E. J., Stow, C. A., Gronewold, A. D., Mason, L. A., McCormick, M. J., Qian, S. S., et al. (2021). Seasonal overturn and stratification changes drive deep-water warming in one of Earth's largest lakes. *Nature Communications*, *12*(1), 1688. https://doi.org/10.1038/s41467-021-21971-1

Biemond, B., Amadori, M., Toffolon, M., Piccolroaz, S., van Haren, H., & Dijkstra, H. A. (2021). Deep-mixing and deep-cooling events in Lake Garda: Simulation and mechanisms. *Journal of Limnology*, *80*(2). https://doi.org/10.4081/jlimnol.2021.2010

Bocaniov, S. A., Ullmann, C., Rinke, K., Lamb, K. G., & Boehrer, B. (2014). Internal waves and mixing in a stratified reservoir: Insights from three-dimensional modeling. *Limnologica*, *49*, 52–67. https://doi.org/10.1016/j.limno.2014.08.004

Boehrer, B., Herzsprung, P., Schultze, M., & Millero, F. J. (2010). Calculating density of water in geochemical lake stratification models. *Limnology and Oceanography: Methods*, *8*(11), 567–574. https://doi.org/10.4319/lom.2010.8.0567

Boehrer, B., & Schultze, M. (2008). Stratification of lakes. *Reviews of Geophysics*, *46*(2). https://doi.org/10.1029/2006RG000210

Boehrer, B., von Rohden, C., & Schultze, M. (2017). Physical features of meromictic lakes: Stratification and circulation. In R. Gulati, E. Zadereev, & A. Degermendzhi (Eds.), *Ecology of meromictic lakes. Ecological studies* (Vol. 228, pp. 15–34). Springer. https://doi.org/10.1007/978-3-319-49143-1_2

Boehrer, B., Yusta, I., Magin, K., & Sanchez-Espana, J. (2016). Quantifying, assessing and removing the extreme gas load from meromictic Guadiana pit lake, Southwest Spain. *Science of the Total Environment*, *1*(563–564), 468–477. https://doi.org/10.1016/j.scitotenv.2016.04.118

Bonomi, G., & Gerletti, M. (1967). Il Lago d'Iseo: Primo quadro limnologico generale (termica, chimica, plancton e benton profondo). *Mem. Ist. Ital. Idrobiol.*, *22*, 149–175.

Bouffard, D., & Wüest, A. (2019). Convection in lakes. *Annual Review of Fluid Mechanics*, *51*(1), 189–215. https://doi.org/10.1146/annurev-fluid-010518-040506

Brizzio, M. C., Garibaldi, L., & Mosello, R. (1999). Evoluzione dell'eutrofizzazione del lago d'Iseo: L'anossia ipolimnetica ed il possibile instaurarsi di condizioni meromittiche. *Atti Associazione Italiana Oceanologia Limnologia*, *13*(1), 91–104.

Butcher, J. B., Nover, D., Johnson, T. E., & Clark, C. M. (2015). Sensitivity of lake thermal and mixing dynamics to climate change. *Climatic Change*, *129*(1–2), 295–305. https://doi.org/10.1007/s10584-015-1326-1

Calamita, E., Lever, J. J., Albergel, C., Woolway, R. I., & Odermatt, D. (2024). Detecting climate-related shifts in lakes: A review of the use of satellite earth observation. *Limnology & Oceanography*, *69*(4), 723–741. https://doi.org/10.1002/lno.12498

Camacho, A., Miracle, M. R., Romero-Viana, L., Picazo, A., End, E., & Vicente, E. (2017). Lake La Cruz, an Iron-rich Karstic meromictic Lake in Central Spain. In R. Gulati, E. Zadereev, & A. Degermendzhi (Eds.), *Ecology of meromictic lakes. Ecological studies* (Vol. 228, pp. 187–233). Springer. https://doi.org/10.1007/978-3-319-49143-1_8

Easterling, D. R., Meehl, G. A., Parmesan, C., Changnon, S. A., Karl, T. R., & Mearns, L. O. (2000). Climate extremes: Observations, modeling, and impacts. *Science*, *289*(5487), 2068–2074. https://doi.org/10.1126/science.289.5487.2068

Ficker, H., Luger, M., Pamminger-Lahnsteiner, B., Achleitner, D., Jagsch, A., & Gassner, H. (2019). Diluting a salty soup: Impact of long-lasting salt pollution on a deep Alpine Lake (Traunsee, Austria) and the downside of recent recovery from salinization. *Aquatic Sciences*, *81*(1), 7. https://doi.org/10.1007/s00027-018-0602-3

Finckh, P. (1981). Heat-flow measurements in 17 peralpine lakes: Summary. *Geological Society of America Bulletin I*, *92*(3), 108–111. https://doi.org/10.1130/0016-7606(1981)92<108:hmipls>2.0.co;2

Garibaldi, L., Brizzio, M. C., Mezzanotte, V., Varallo, A., & Mosello, R. (1995). The continuing evolution of Lake Iseo (N. Italy): The appearance of anoxia. *Mem. Ist. Ital. Idrobiol.*, *53*, 191–212.

Ghane, A., & Boegman, L. (2021). Turnover in a small Canadian Shield lake. *Limnology & Oceanography*, *66*(9), 3356. https://doi.org/10.1002/Lno.11884

Gobiet, A., Kotlarski, S., Beniston, M., Heinrich, G., Rajczak, J., & Stoffel, M. (2014). 21st century climate change in the European Alps—A review. *Science of the Total Environment*, *493*, 1138–1151. https://doi.org/10.1016/j.scitotenv.2013.07.050

Idso, S. B. (1973). On the concept of lake stability. *Limnology & Oceanography*, *18*(4), 681–683. https://doi.org/10.4319/lo.1973.18.4.0681

Imberger, J., & Patterson, J. (1990). Physical limnology. *Advances in Applied Mechanics*, *27*, 303–475. https://doi.org/10.1016/S0065-2156(08)70199-6

Katsev, S., Verburg, P., Llirós, M., Minor, E. C., Kruger, B. R., & Li, J. (2017). Tropical meromictic lakes: Specifics of meromixis and case studies of Lakes Tanganyika, Malawi, and Matano. In R. Gulati, E. Zadereev, & A. Degermendzhi (Eds.), *Ecology of meromictic lakes. Ecological studies* (Vol. 228). Springer. https://doi.org/10.1007/978-3-319-49143-1_10

Kraemer, B. M., Anneville, O., Chandra, S., Dix, M., Kuusisto, E., Livingstone, D. M., et al. (2015). Morphometry and average temperature affect lake stratification responses to climate change. *Geophysical Research Letters*, *42*(12), 4981–4988. https://doi.org/10.1002/2015GL064097

Lau, M. P., Valerio, G., Pilotti, M., & Hupfer M, M. (2020). Intermittent meromixis controls the trophic state of warming deep lakes. *Scientific Reports*, *10*(1), 12928. https://doi.org/10.1038/s41598-020-69721-5

Lemmin, U. (2020). Insights into the dynamics of the deep hypolimnion of Lake Geneva as revealed by long-term temperature, oxygen, and current measurements. *Limnology & Oceanography*, *65*(9), 2092–2107. https://doi.org/10.1002/lno.11441

Livingstone, D. M. (1997). An example of the simultaneous occurrence of climate-driven "saw-tooth" deep-water warming/cooling episodes in several Swiss lakes. *Verh Internat Verein Limnol*, *26*(2), 822–828. https://doi.org/10.1080/03680770.1995.11900832

Many, G., Escoffier, N., Perolo, P., Bärenbold, F., Bouffard, D., & Perga, M. E. (2024). Calcite precipitation: The forgotten piece of lakes' carbon cycle. *Science Advances*, *10*(44). https://doi.org/10.1126/sciadv.ado5924

Monismith, S. G. (1986). An experimental study of the upwelling response of stratified reservoirs to surface shear stress. *Journal of Fluid Mechanics*, *171*, 407–439. https://doi.org/10.1017/S0022112086001507

Monti, R. (1929). Limnologia comparata dei laghi insubrici. *SIL Proceedings, 1922–2010*, *4*(1), 462–497. https://doi.org/10.1080/03680770.1929.11898422

Moreira, S., Schultze, M., Rahn, K., & Boehrer, B. (2016). A practical approach to lake water density from electrical conductivity and temperature. *Hydrology and Earth System Sciences*, *20*(7), 2975–2986. https://doi.org/10.5194/hess-20-2975-2016

North, R. P., North, R. L., Livingstone, D. M., Köster, O., & Kipfer, R. (2014). Long-term changes in hypoxia and soluble reactive phosphorus in the hypolimnion of a large temperate lake: Consequences of a climate regime shift. *Global Change Biology*, *20*(3), 811–823. https://doi.org/10.1111/gcb.12371

O'Reilly, C. M., Alin, S. R., Plisnier, P. D., Cohen, A. S., & McKee, B. A. (2003). Climate change decreases aquatic ecosystem productivity of Lake Tanganyika, Africa. *Nature*, *424*(6950), 766–768. https://doi.org/10.1038/nature01833

Peng, N., Lemmin, U., Mettra, F., Reiss, R. S., & Barry, D. A. (2024). Deepwater renewal in a large, deep lake (Lake Geneva): Identifying and quantifying winter cooling processes using heat budget decomposition. *Water Resources Research*, *60*(4), e2023WR034936. https://doi.org/10.1029/2023WR034936

Pieters, R., & Lawrence, G. A. (2014). Physical processes and meromixis in pit lakes subject to ice cover. *Canadian Journal of Civil Engineering*, *41*(6), 569–578. https://doi.org/10.1139/cjce-2012-0132

Pilotti, M., Barone, L., Balistrocchi, M., Valerio, G., Milanesi, L., & Nizzoli, D. (2021). Nutrient delivery efficiency of a combined sewer along a lake challenged by incipient eutrophication. *Water Research*, *190*, art. 116727. https://doi.org/10.1016/j.watres.2020.116727

Pilotti, M., Valerio, G., Giardino, C., Bresciani, M., & Chapra, S. (2018). Evidence from field measurements and satellite imaging of impact of Earth rotation on Lake Iseo chemistry. *Journal of Great Lakes Research*, *44*(1), 14–25. https://doi.org/10.1016/j.jglr.2017.10.005

Pilotti, M., Valerio, G., & Leoni, B. (2013). Data set for hydrodynamic lake model calibration: A deep prealpine case. *Water Resources Research*, *49*(10), 1–5. https://doi.org/10.1002/wrcr.20506

Rainato, R., Martini, L., Pellegrini, G., & Picco, L. (2021). Hydrological, geomorphic and sedimentological responses of an alpine basin to a severe weather event (Vaia storm). *Catena*, *207*, 105600. https://doi.org/10.1016/j.catena.2021.105600

Robertson, D. M., & Imberger, J. (1994). Lake Number, a quantitative indicator of mixing used to estimate changes in dissolved oxygen. *International Review of Hydrobiology*, *79*(2), 159–176. https://doi.org/10.1002/iroh.19940790202

Rogora, M., Buzzi, F., Dresdi, C., Leoni, B., Lepori, F., Mosello, R., et al. (2018). Climatic effects on vertical mixing and deep-water oxygen content in the subalpine lakes in Italy. *Hydrobiologia*, *824*(1), 33–50. https://doi.org/10.1007/s10750-018-3623-y

Schindler, D. W., & Vallentyne, J. R. (2008). *The algal bowl: Overfertilization of the world's freshwaters and estuaries*. The University of Alberta Press. 334.

Schladow, S. G., Pálmarsson, S. Ó., Steissberg, T. E., Hook, S. J., & Prata, F. E. (2004). An extraordinary upwelling event in a deep thermally stratified lake. *Geophysical Research Letters*, *31*(15), L15504. https://doi.org/10.1029/2004GL020392

Schultze, M., Boehrer, B., Wendt-Potthoff, K., Sánchez-España, J., & Castendyk, D. (2017). Meromictic pit lakes: Case studies from Spain, Germany and Canada and general aspects of management and modelling. In R. Gulati, E. Zadereev, & A. Degermendzhi (Eds.), *Ecology of meromictic lakes. Ecological studies* (Vol. 228, pp. 235–275). Springer. https://doi.org/10.1007/978-3-319-49143-1_9

Stevens, C., & Imberger, J. (1996). The initial response of a stratified lake to a surface shear stress. *Journal of Fluid Mechanics*, *312*, 39–66. https://doi.org/10.1017/S0022112096001917

Tanaka, M., Girard, G., Davis, R., Peuto, A., & Bignell, N. (2001). Recommended table for the density of water between 0∘C and 40∘C based on recent experimental reports. *Metrologia*, *38*(4), 301–309. https://doi.org/10.1088/0026-1394/38/4/3

Valerio, G., Cantelli, A., Monti, P., & Leuzzi, G. (2017). A modeling approach to identify the effective forcing exerted by wind on a prealpine lake surrounded by a complex topography. *Water Resources Research*, *53*(5), 4036–4052. https://doi.org/10.1002/2016WR020335

Valerio, G., Pilotti, M., Lau, M. P., & Hupfer, M. (2019). Oxycline oscillations induced by internal waves in deep Lake Iseo. *Hydrology and Earth System Sciences*, *23*(3), 1763–1777. https://doi.org/10.5194/hess-23-1763-2019

Verburg, P., & Antenucci, J. P. (2010). Persistent unstable atmospheric boundary layer enhances sensible and latent heat loss in a tropical great lake: Lake Tanganyika. *Journal of Geophysical Research*, *115*(D11), D11109. https://doi.org/10.1029/2009JD012839

Verburg, P., & Hecky, R. E. (2009). The physics of the warming of Lake Tanganyika by climate change. *Limnology & Oceanography*, *54*(6_part_2), 2418–2430. https://doi.org/10.4319/lo.2009.54.6_part_2.2418

Wahl, B., & Peeters, F. (2014). Effect of climatic changes on stratification and deep-water renewal in Lake Constance assessed by sensitivity studies with a 3D hydrodynamic model. *Limnology & Oceanography*, *59*(3), 1035–1052. https://doi.org/10.4319/lo.2014.59.3.1035

Wetzel, R. G. (2001). *Limnology: Lake and river ecosystems*. Academic Press.

Woolway, R. I., Kraemer, B. M., Lenters, J. D., Merchant, C. J., O'Reilly, C. M., & Sharma, S. (2020). Global lake responses to climate change. *Nature Reviews Earth & Environment*, *1*(8), 388–403. https://doi.org/10.1038/s43017-020-0067-5

Woolway, R. I., & Merchant, C. J. (2019). Worldwide alteration of lake mixing regimes in response to climate change. *Nature Geoscience*, *12*(4), 271–276. https://doi.org/10.1038/s41561-019-0322-x

Xu, L., Yuan, S., Tang, H., Qiu, J., Xiao, Y., Whittaker, C., & Gualtieri, C. (2022). Mixing dynamics at the large confluence between the Yangtze River and Poyang Lake. *Water Resources Research*, *58*(11), art. e2022WR032195. https://doi.org/10.1029/2022WR032195

Yankova, Y., Neuenschwander, S., Köster, O., & Posch, T. (2017). Abrupt stop of deep water turnover with lake warming: Drastic consequences for algal primary producers. *Scientific Reports*, *7*(1), art. 13770. https://doi.org/10.1038/s41598-017-13159-9